Drug Design, Development and Therapy

Dovepress
Taylor & Francis Group

Open Access Full Text Article

ORIGINAL RESEARCH

# Nanoencapsulated α-Mangostin Loaded Chitosan-Alginate Hydrogel Films for Enhanced Topical Anti Acne Therapy

Nia Yuniarsih[1,2], Anis Yohana Chaerunisaa[3], Ahmed Fouad Abdelwahab Mohammed[4,5], Khaled M Elamin[6], Muchtaridi Muchtaridi[7], Nasrul Wathoni[3]

[1]Doctoral Program of Pharmacy, Department of Pharmaceutics and Pharmaceutical Technology, Faculty of Pharmacy, Padjadjaran University, Sumedang, 45363, Indonesia; [2]Faculty of Pharmacy, Universitas Jenderal Achmad Yani, Cimahi, 40533, Indonesia; [3]Department of Pharmaceutics and Pharmaceutical Technology Faculty of Pharmacy, Padjadjaran University, Sumedang, 45363, Indonesia; [4]Department of Pharmaceutics, Faculty of Pharmacy, Minia University, Minia, 61519, Egypt; [5]Department of Pharmaceutics, Faculty of Pharmacy, Minia National University, New Minia, 61768, Egypt; [6]Graduate School of Pharmaceutical Sciences, Kumamoto University, Kumamoto, 862-0973, Japan; [7]Department of Pharmaceutical Analysis and Medicinal Chemistry, Faculty of Pharmacy, Padjadjaran University, Sumedang, 45363, Indonesia

Correspondence: Nasrul Wathoni, Department of Pharmaceutics and Pharmaceutical Technology, Faculty of Pharmacy, Padjadjaran University, Sumedang, 45363, Indonesia, Tel/Fax+62-22-842-888-888, Email nasrul@unpad.ac.id



**Background:** α-Mangostin (α-M) is a natural antimicrobial and anti-inflammatory compound with promising anti-acne potential; however, its poor solubility and instability limit its topical use. This study developed and evaluated chitosan-alginate hydrogel films incorporating nanoencapsulated α-M (HF α-M NPs) to enhance stability, skin penetration, and therapeutic efficacy against *Propionibacterium acnes*.

**Methods:** α-M NPs were produced by ionic gelation using chitosan and sodium tripolyphosphate, followed by alginate coating, and subsequently incorporated into chitosan-alginate hydrogel films. Nanoparticles and films were characterized using SEM, FTIR, mechanical testing, swelling behavior, degradability analysis, and in vitro drug-release studies. The anti-acne performance was assessed in a *P. acnes* mouse model using total plate count, histopathological evaluation, and measurement of edema and erythema.

**Results:** The nanoparticles exhibited a mean size of 229.7 ± 18.15 nm, PDI of 0.450 ± 0.046, and zeta potential of +40.9 ± 1.91 mV, indicating strong colloidal stability. SEM confirmed the uniform distribution of nanoparticle in the hydrogel matrix, while FTIR revealed molecular interactions between the polymers and α-M. HF α-M NPs showed improved mechanical strength, controlled swelling, and a sustained release profile compared with free α-M films. In vivo, the HF α-M NPs achieved the greatest reduction in *P. acnes* load ($2.46 \times 10^1$ CFU/g), significant epithelial restoration, and the lowest edema and erythema scores, which were superior to those of free α-M and comparable to those of clindamycin gel.

**Conclusion:** Nanoencapsulation of α-M within a chitosan-alginate hydrogel matrix significantly enhanced its stability, release behavior, and antimicrobial and anti-inflammatory effects. HF α-M NPs represents a promising antibiotic free topical therapy for acne and merits further optimization and clinical investigation.

**Keywords:** α-mangostin, chitosan-alginate nanoparticles, hydrogel film, Propionibacterium acnes, topical delivery, anti-acne therapy

## Introduction

Acne (*acne vulgaris*) is a very common condition of skin issue, particularly among young adults and adolescents. Epidemiological studies estimate that approximately 85% of adolescents and young adults experience acne, with a notable prevalence persisting into adulthood.[1] It is one of the most prevalent skin conditions globally, affecting approximately 9.4% of the population, making it the eighth most common disease worldwide.[2] This condition is influenced by sebum hyperproduction, hyper keratinization, proliferation of *Propionibacterium acnes* (*P. acnes*), and inflammation of the hair follicles. The presence of acne can reduce self-esteem and self-confidence; therefore, an effective treatment is beneficial to quality of life for adolescents. Conventional treatments often involve retinoids,

https://doi.org/10.2147/DDDT.S588115
Received: 11 December 2025
Accepted: 20 February 2026
Published: 12 March 2026

antibiotics, and benzoyl peroxide but are often accompanied by side effects and microorganism resistance.[3,4] Therefore, the development of effective and safe topical formulations to suppress inflammation and reduce the population of *P. acnes* is urgently required. Alpha-mangostin (α-M), an active compound from mangosteen (*Garcinia mangostana*), is known to have strong activities of anti-inflammatory, antioxidant, and antimicrobial, thereby positioning it as a possible agent for anti-acne.[5,6] However, α-M is characterized by poor target selectivity and low water solubility in the human body.[7] The use of nano-emulsions or nanoparticles of alpha-mangostin (α-M NPs) has been shown to topically increase its penetration and stability.[6,8,9] Moreover, another study found that 5% α-M gel was effective in treating acne vulgaris, showing comparable effects to 1% clindamycin gel for comedowns, inflammatory lesion reduction, clinical assessment, porphyrin levels, and *P. acnes* eradication over a 12-week treatment course.[10] This aligns with studies linking sebaceous glands to hair follicles and utilizing cellulose-based nanoparticles as nano-reservoirs, demonstrating significant improvements in α-M-treated acne vulgaris.[6,11] A range of nano-drug delivery systems has been developed for acne therapy, such as lipid nanocarriers consisting of NLCs (nanostructured lipid carriers),[12,13] solid lipid nanoparticles,[14,15] nano-emulsions,[16] liposomes,[17] polymeric nano micelles, and microemulsions.[15,18] The incorporation of α-M nanoparticles within chitosan-alginate hydrogel films not only improves the therapeutic efficacy against acne but also addresses the increasing concerns surrounding the side effects of conventional treatments.[11] Recent studies have shown that chitosan and alginate, as natural polymers, exhibit biodegradability and biocompatibility, thereby rendering them ideal for drug delivery systems in dermatological applications.[19,20] In addition, chitosan exhibits intrinsic antimicrobial activity through electrostatic interactions between its positively charged amino groups and negatively charged bacterial cell membranes, leading to disruption of cell wall integrity and inhibition of microbial growth.[21,22] This inherent antimicrobial property may act synergistically with α-M, thereby enhancing overall antibacterial effectiveness against acne-associated pathogens while reducing reliance on high doses of conventional antibiotics.[23,24] However, the creation of a delivery system that can increase bioavailability while providing hydration and protective effects to the skin is still needed.

The skin acts as a barrier for transdermal drug delivery, and penetration enhancers lower stratum corneum integrity by causing a transient and reversible disruption of the highly ordered structure.[25] Optimally, a permeation enhancer should be safe, non-irritant, and non-toxic, and should result in a reversible and rapid enhancement in skin permeability.[26]

Generally, acne patches already on the market incorporate hydrocolloid-synthesizing agents. Acne patches that available are commonly composed of hydrogels or hydrocolloids.

Substances are recognized for their application in medical dressings.[27] Hydrocolloid dressings comprise two layers: a colloid layer and a waterproof layer. The colloid layer is the inner layer, while the water-impermeable layer is positioned on the outside. The water-impermeable layer served as a protective layer and aid in preventing the spread of pathogenic microorganisms; however, this water-impermeable layer is able to promote the growth of *P. acnes* by inducing hypoxic conditions.[28] Medicated acne patches are also referred to as hydrogel patches since they incorporate active ingredients that can eliminate acne-causing bacteria. The hydrocolloid patch is able to absorb fluid from the pimples, flattening them.[29] Based on the test of in vitro antibacterial, the patch is not only efficacious on the skin underneath but also on the surrounding skin. This patch can also be removed from the skin without causing pain, even though it adheres well to the facial skin.[28] Release systems extend the interval between acne treatment and drug release, determining their effectiveness. Cross-linking in film forming techniques plays a significant role in controlling the drug release rate.[11] Drug delivery systems are often developed from naturally occurring polymers that can be easily cross-linked ionically, including the cationic polymer chitosan as well as anionic polysaccharides like sodium alginate.[8,30,31] Various degradable natural polymers have been utilized in research and medical applications, including alginate, chitosan, gelatin, and cellulose derived polymers such as ethyl cellulose, sodium carboxymethylcellulose, and hydroxypropyl methylcellulose.[32,33] A hydrogel matrix from the combination of alginate and chitosan provides biocompatibility, biodegradability, and the ability to effectively retain drugs.[19,24] In addition, the antimicrobial and skin-penetrating properties of chitosan are beneficial for acne therapy.[34] The incorporation of α-M NPs into chitosan-alginate based hydrogels is expected to enhance the efficacy of topical anti-acne treatments.[6,35] Glycerin can absorb and retain moisture, helping to relieve dry skin and promote faster healing of acne.[29] The design, characterization, and in vivo as well as in vitro evaluations of α-M NPs hydrogel films aimed to guarantee the formulation's effectiveness and safety. Parameters such as nanoparticle size, swelling, tensile strength, surface charge, and drug release are important for determining the

success of this delivery system. In addition, antimicrobial activity testing against *P. acnes* and skin irritation testing should be performed as part of the initial evaluation of the formulation. The implementation of design studies, characterization, and in vivo and in vitro evaluations will provide a strong scientific basis for future clinical applications. This innovative approach not only improved the sustained release of the active compound but also maximized skin penetration, thereby increasing the overall effectiveness of treatment. From a translational perspective, the proposed delivery system may offer advantages for clinical development, including improved efficacy at lower doses and the potential to reduce adverse effects associated with conventional therapies. Furthermore, the use of biocompatible and scalable polymeric materials supports the feasibility of future commercialization, particularly for topical dermatological products requiring controlled drug delivery and patient-friendly application.

# Materials and Methods

## Materials

α-M was sourced from Chengdu Biopurify Phytochemicals (Sichuan, China). As the primary base polymer, Chitosan was obtained with a 70% purity. Sodium tripolyphosphate was used as the cross-linker. The coating polymer sodium alginate was acquired from Wako Pure Chemical Industries (Tokyo, Japan), and ethanol and potassium bromide (KBr) were purchased from CV. Kristata (West Java, Indonesia) and PT. Merck (West Java, Indonesia). *Propionibacterium acnes* (ATCC 11827) (Biomerieux, Indonesia).

## Animals

The Ethical Committee for the Experimental Use of Animals Research Ethics Committee at Universitas Jendral Achmad Yani approved the experimental procedures, which were performed following the National Institutes of Health's guidelines for the care and use of laboratory animals. The Experimental Animal Center of the Food and Drug Research Agency of the Republic of Indonesia (Jakarta, Indonesia) provided 180–220 g Sprague-Dawley (SD) rats. The animals were maintained in climate-controlled environments with *ad libitum* access to water and food, a 12-h light/dark cycle, temperatures of 22°C-26°C, as well as humidity of 40% and 70% (approval No. 10015/KEP-UNJANI/VI/2024).

## Preparation of Chitosan Alginate-Based NPs α-M Loaded Hydrogel Film

### Preparation of α-M Loaded Chitosan Alginate Nanoparticles (α-M NPs)

Ionic gelation combined with a microvolume flow titration technique was employed to prepare polymeric nanoparticles composed of α-mangostin (α-M), chitosan, sodium alginate, and sodium tripolyphosphate (Na-TPP) as the crosslinking agent (Table 1). Initially, α-M (30 mg) was dissolved in absolute ethanol (10 mL) to obtain a clear solution. Chitosan solution was prepared by dissolving 100 mg of chitosan in 10 mL of 1% (v/v) acetic acid, followed by dilution with distilled water to a final volume of 100 mL, and the pH was adjusted to 3. Separately, a Na-TPP solution was prepared by dissolving 2.5 mg of Na-TPP in 20 mL of distilled water and adjusting the pH to 8. Sodium alginate solution was prepared by dissolving 10 mg of sodium alginate in 10 mL of distilled water under continuous stirring until complete homogenization was achieved. The α-M solution was then added dropwise into the chitosan solution using a microvolume syringe pump (KD Scientific KDS 200) at a controlled flow rate of 0.5 mL/min under continuous stirring at 600 rpm and a temperature of 40 °C. After a homogeneous dispersion was formed, the Na-TPP solution was introduced dropwise under identical conditions to induce ionic gelation between chitosan and Na-TPP. Subsequently, the alginate solution was added to form an outer alginate layer on the nanoparticle surface. The alginate coating step was

**Table 1** Formulation of α-M NPs

| Components | Concentration |
|---|---|
| α-M | 0.03% |
| Chitosan | 0.3% |
| Sodium Alginate | 0.01% |
| Sodium Tripolyphosphate | 0.06 |

 https://doi.org/10.2147/DDDT.S588115 

performed using a microvolume flow titration approach, in which both the droplet volume and flow rate were precisely controlled, enabling the formation of fine and uniform droplets and thereby improving nanoparticle homogeneity. The resulting dispersion was further processed by probe sonication at an output power of approximately 200 W (50% amplitude) with a duty cycle of 0.5 (pulse mode: 5 s on/5 s off) for 1 h to reduce particle size and enhance uniformity. Finally, the nanoparticle suspension was spray-dried using a Büchi B-290 spray dryer at an inlet temperature of 80 °C and an airflow rate of 5 L/min to obtain dry α-M loaded chitosan-alginate nanoparticle powder.[8,36]

### Preparation of Alginate-Chitosan Hydrogel Film (HF)

The alginate-chitosan hydrogel film was prepared according to the composition presented in Table 2, beginning with the preparation of individual polymer solutions. An alginate solution was formulated by slowly incorporating alginate powder into distilled water with constant stirring at room temperature. To prepare the chitosan solution, chitosan powder was dissolved in a measured volume of distilled water and stirred for 45 minutes. The alginate solution was subsequently incorporated in a dropwise manner to the chitosan solution with constant stirring. After complete mixing of both solutions, glycerin was incorporated as a plasticizer, and the mixture was agitated for a further 30 minutes to achieve a hydrogel solution that homogeneous. The resulting solution was cast into a polypropylene box and leveled to a uniform thickness of 2–4 mm in the box. The hydrogel was subsequently dried for 24 h at 60 °C. Once dried, the film was cut into circular discs with a surface area of 1 $cm^2$.[24,37]

### Preparation of Chitosan-Alginate Hydrogel Films Incorporating α-M NPs (HF α-M NPs)

Chitosan-alginate hydrogel films (1 $cm^2$) were prepared for drug loading. A nanoparticle suspension of α-M (250 ug/10 µL) was prepared using glycerin as the dispersing agent. The suspension was applied to the surface of the hydrogel films using a micropipette to ensure even distribution. The loaded films were subjected to incubation for 24 hours at 4 °C to facilitate absorption as well as stabilization, thereafter dried for 1 hour at 37 °C to remove residual moisture.[19,24]

## Characterization of HF α-M NPs Based on Chitosan-Alginate

### Scanning Electron Microscopy

The surface morphology of the HF α-M NPs was examined using SEM (scanning electron microscopy) (Model SU3500 SEM; Hitachi, Tokyo, Japan). The surface morphology of the films was inspected using a Jeol JSM-IT300 instrument with a 20 kV operating voltage. The HF α-M NPs samples were mounted on a sample holder and plated with gold-palladium over 10 seconds. The SEM micrographs were acquired at working distances of 8.4–13.4 millimeters with × 100 and x15.000 magnification. Images were recorded from 5 distinct regions of the films to assess the microstructure consistency.[20,38,39]

### Fourier Transform Infra-Red

The interactions between the functional groups of α-M and other ingredients in the polymeric nanoparticle system were examined using FTIR (Fourier-transform infrared) spectroscopy (IR Prestige-21; Shimadzu, Kyoto, Japan). HF α-M NPs were blended with 200 mg KBr, the pellets were molded with vacuum pressure (60 kN within 15 minutes), and assessed at 4000–400 $cm^{-1}$. The interaction was illustrated by contrasting the functional groups of the polymeric nanoparticle system with those of pure α-M.[40]

**Table 2** Formulation of HF α-M NPs

| Components | Sod. Alginat (g) | Chitosan (g) | Glycerin (% w/v) | Acetic Acid (mL) | α-M (ug) | α-M NPs (ug) |
|---|---|---|---|---|---|---|
| HF | 0,5 | 0,1 | 0,1 | 5 | - | - |
| HF α-M | 0,5 | 0,1 | 0,1 | 5 | 250 | - |
| HF α-M NPs | 0,5 | 0,1 | 0,1 | 5 | - | 250 |

## Weight and Thickness

The weights of the hydrogel films (HF α-M NPs) were quantified with an analytical balance, and their thicknesses were gauged utilizing Vernier's calipers. The HF α-M NPs sample test was replicated at five distinct positions on the film with 0.001 mm accuracy.[20,39,41] The experiments were performed in five replicates each. The results are displayed as the mean ± standard error of the mean (SEM).

## Degradability Study

The hydrogel film (1 $cm^2$) was quantified for weight, submerged in 2 mL of 20% TCA solution, and held for 24 h. The TCA solution was removed and re-weighed until it reached a constant state. The degradability of the trypsin solution was also examined utilizing an identical procedure.[33,36] The experiments were performed in five replicates each. The results are displayed as the mean ± standard error of the mean (SEM). The percent change in weight was derived with the equation below:

$$\text{Percent change in weight } = \frac{\text{Final weight}}{\text{Initial weight}} \times 100$$

## Mechanical Strength

The TS (tensile strength) and EB (elongation at break) were estimated utilizing a Tensile Tester (Zwick Roell) in accordance with the ASTM standard method D1822 at a 10 mm/min stretching rate and a 0.05 MPa preload. The HF NPs α–M were trimmed to dimensions of 3×2 cm.[39] The experiments were performed in five replicates each. The results are displayed as the mean ± standard error of the mean (SEM). The TS and EB values were computed according to the equations below:

$$\text{TS}\left(\text{N}/\text{mm}^2\right) = \frac{\text{Force at break(N)}}{\text{Initial cross sectional area(mm2)}}$$

$$\text{EB}(\%) = \frac{\text{Increase in lenght (mm) at break}}{\text{Initial film lenght (mm)}} \times 100$$

## Swelling Degree

The hydrogel film (1 $cm^2$) was submerged in phosphate-buffered saline (25 mL) at room temperature (pH 7.4). After 1, 4, and 6 h, the sample was gently withdrawn from the buffer solution, excess buffer on its surface was blotted utilizing filter paper, as well as the sample was reweighed. The degree of swelling was estimated using the equation below:

$$\%\ \text{swelling degree } = \frac{\text{Ws} - \text{Wd}}{\text{Wd}} \times 100$$

where Ws represents the weight of the swollen film at a specific time and Wd indicates the weight of the first film (the dried film). The experiments were performed in five replicates each. The results are displayed as the mean ± standard error of the mean (SEM).

## In vitro Release Study

In these experiments, the paddle-over disk method (USP apparatus V) was employed for estimating drug release from the prepared batches. Dry films of known clear-cut shapes with thickness and weight variables were placed over a glass plate with a bonding agent. A glass plate was placed in 500 mL of phosphate buffer (pH 7.4) serving as the dissolution medium, which was maintained at 32 ± 0.5 °C. The paddle was positioned 2.5 cm above the glass plate and operated at a rotation speed of 50 rpm. The paddle was placed 2.5 cm from the beaker plate and operated at a rate of 50 rpm. The Sample (5 mL aliquots) was reserved at suitable time intervals over a 24-h period and evaluated utilizing UV spectrophotometry at 246 nm wavelength.[42] The experiments were performed in five replicates each. The results are displayed as the mean ± standard error of the mean (SEM).

# In vivo Antimicrobial Activity

## Animal Grouping, Modeling, and Administration

Five groups of 25 SD rats were randomly allocated to: regular control, model experiment (HF α-M NPS), HF α-M, positive control (received clindamycin gel), and negative control (received HF) (Table 3). Every group comprised five rats each. With the exception of the normal control, the other five groups were administered daily intradermal injections of *P. acnes* for three days on the back. Immediately before injection, *P. acnes* was mixed with aqua pro injection ($10^8$ CFU/mL). Subsequently, the mixture (0.5 mL) was intradermally injected into the back of each rat. On the fourth day, HF was applied twice daily for four consecutive days on the injected skin area.[43–45] Effective establishment of the acne model was evidenced by pronounced erythema, thickening, swelling, nodules, sebum, and induration on the skin surface at the modeling sites. After 4 days of HF application, the papules were excised with an 8 mm biopsy punch. In this study, a total plate count test was executed to measure the number of remaining *P. acnes*. The papules were then dripped with 1 mL of sterile PBS solution, the liquid was collected, and 10 mL of sterile PBS was added. Then, 10 mcl was planted in blood agar media and subjected to incubation at 37 °C for 24 h in anaerobic gas-producing bags. A 10 mL stock solution was prepared, and multilevel dilution was performed. For each dilution, 15 mL of NA medium at 45 °C was added, homogenized, and allowed to cool and solidify. Gram-positive staining was then performed to ensure the growth of *P. acnes* bacteria.[43]

## Calculation of Total Bacterial Plate Count

The number of colonies that grew was calculated after incubation for 1×24 h; both single colonies and colonies that merged were considered as one bacterial colony.[46,47]

The number of bacteria that met the requirements for counting ranges from to 30–300 colonies.

If the total of colonies was <30, it was considered too few (did not meet requirements).

If the total of colonies is >300, it is also considered too many (does not meet the requirements).

The method for calculating ALT is as follows

$$\text{ALT bacteria} = \frac{1}{\text{Dilution factor}} \times \text{Number of colonies}$$

## Histopathological Analysis

Histopathological analysis was performed after injecting *P. acnes* into the affected papules. The papules were submerged in 10 percents NBF (Neutral Buffered Formalin) to avoid spoilage. The tissues were subsequently blocked with paraffin and sectioned to a thickness of 3–5 μm utilizing a microtome (Leica RM 2235, United States). The slices were prepared for immunohistochemistry utilizing HE (hematoxylin and eosin) staining and examined under an Olympus microscope. The parameter evaluated was the development of an epithelial layer within the tissue.[48–50] Epithelial thickness was quantified utilizing ImageJ® software.

**Table 3** Experimental Animal Groups

| Group | Treatment Description |
|---|---|
| Group 1 (Normal) | No treatment was administered. |
| Group 2 (Negative Control/NC) | *P. acnes* were applied together with the hydrogel film base. |
| Group 3 (Positive Control/ PC) | *P. acnes* were applied together with Clindamycin gel. |
| Group 4 (HF α-M) | *P. acnes* were applied together with hydrogel film containing α-M. |
| Group 5 (HF α-M NPs). | *P. acnes* were applied together with hydrogel film containing nano α-M. |

## Statistical Analysis

All experiments were replicated a minimum of five independent trials. Values are shown as mean ± standard error of the mean (SEM). Differences between means of the parameters measured were compared utilizing Two-way analysis of variance continued with Tukey's post hoc test employing GraphPad Prism version 8. A $p < 0.05$ value was deemed significant.

# Results

## Preparation of Polymeric NPs

All components in the polymeric nanoparticle system (polymer concentrations and active pharmaceutical ingredients) were selected guided by the literature, and the optimization procedures were defined (Table 1).

## Characterization of Nanoparticles

The chitosan alginate-based α-M NPs exhibited an average particle size of 229.7 ± 18.15 nm, zeta potential of 40.9 ± 1.91 mV, as well as PDI of 0.450 ± 0.046 (Table 4). The nanoscale size confirms successful formation through ionic gelation and ultrasonic dispersion, consistent with previous chitosan-alginate systems.[8] Particle sizes within 100–500 nm are suitable for topical penetration, enabling nanoparticles to reach sebaceous follicles, the primary colonization site of *P. acnes*.[51] A moderate PDI (<0.5) indicates a relatively homogeneous size distribution, which supports formulation stability and uniform drug release.[52,53] The high positive zeta potential (+40.9 mV) demonstrated excellent colloidal stability and prevented aggregation during storage.

### Formulation of Chitosan-Alginate Hydrogel Films Incorporating α-M NPs (HF α-M NPs)

The chitosan-alginate hydrogel films were successfully formulated in HF, α-M HF, and HF α-M NPs according to the compositions presented in Table 2. All formulations contained identical base components, including sodium alginate (0.5 g), chitosan (0.1 g), glycerin (0.1% w/v), and acetic acid (5 mL), ensuring consistent polymeric matrix characteristics across groups. For the α-M HF formulation, free α-M (250 µg) was directly incorporated into the film-forming dispersion. In contrast, the HF α-M NPs formulation was prepared by integrating 250 µg of preformed α-M nanoparticles into the hydrogel matrix. Visual and structural observations of the resulting hydrogel films demonstrated that all formulations possessed a clear, flexible, and homogeneous appearance without visible phase separation (Figure 1), indicating successful polymer blending and plasticization. The uniformity of the hydrogel films and successful incorporation of either free drug or nanoparticles suggest that the chitosan-alginate network provides an effective entrapment capacity for both forms of α-M, making the system suitable for subsequent characterization and topical-delivery assessment.

## Characterization of HF NPs α- M Based on Chitosan-Alginate

### Macroscopic and Microscopic Morphological Analyses

Macroscopic and microscopic morphological analyses provided important insights into the physical characteristics of the formulated HF in Figure 1 (Figure 1). Macroscopically (Figure 1A), HF without α-M exhibited a homogeneous pale white surface, whereas the addition of α-M resulted in a yellowish color change. Furthermore, the incorporation of α-M NPs into the hydrogel film produced a golden-brown color, reflecting the successful integration of the active compound into the chitosan-alginate polymer matrix. Microscopic observations using SEM at 20,000 × magnification revealed clear differences between the formulations (Figure 1B). The control HF sample exhibited a relatively smooth surface without any distributed particles. In contrast, α-M HF exhibited a rougher surface with small aggregates, indicating that free α-M is prone to crystallization or uneven distribution within the polymer matrix.

**Table 4** Results of Particle Size, PDI and Zeta Potential of α-M NPs

| Particle Size | PDI (Polydispersity Index) | Zeta Potential |
|---|---|---|
| 229.7 nm ± 18.15 | 0.450± 0.046 | 40.9 mv ±1.91 |


https://doi.org/10.2147/DDDT.S588115

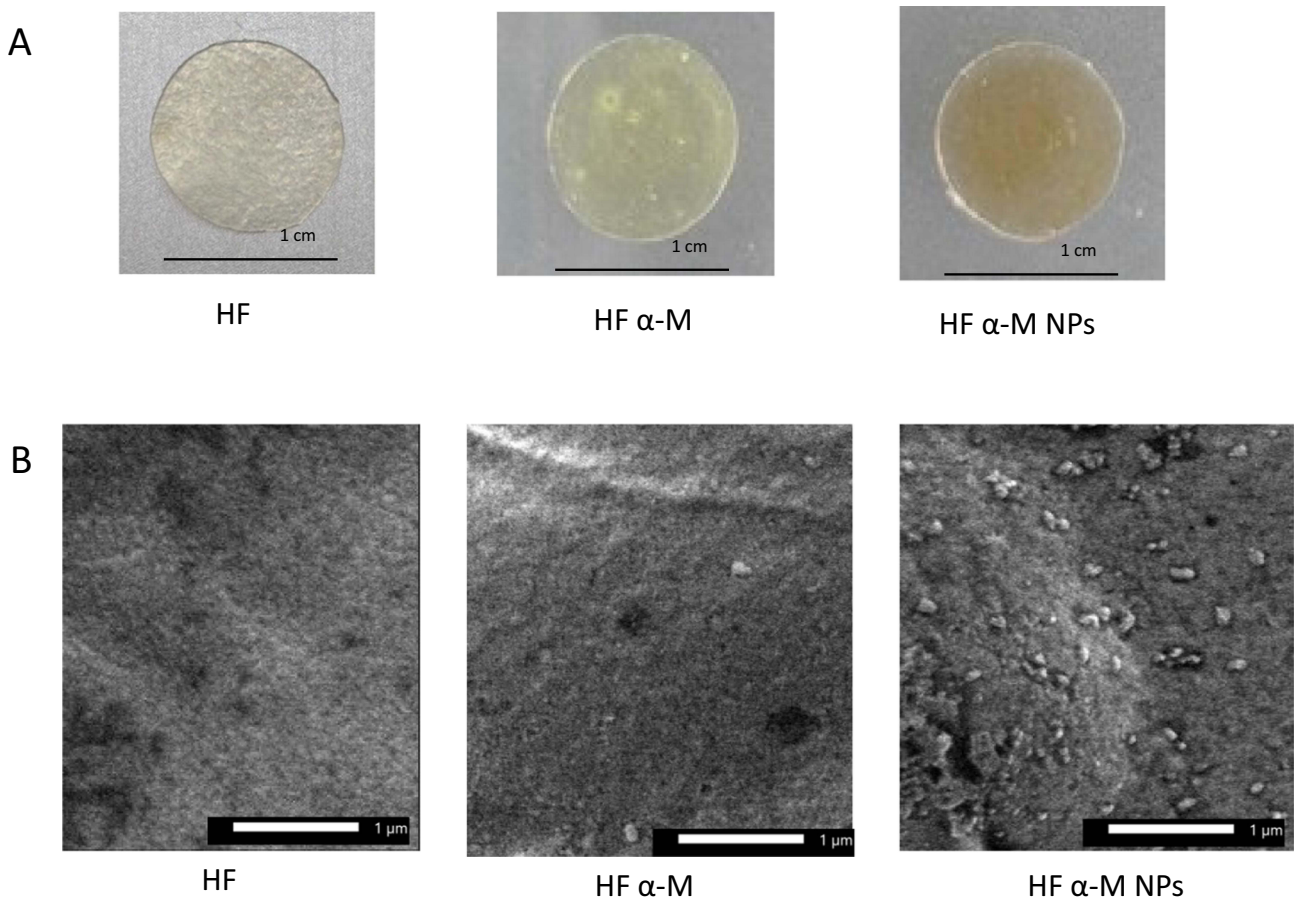


**Figure 1** Physical appearances of HF, HF α-M, and HF α-M NPs: Macroscopic (**A**) and microscopic at 20.000 x magnification (**B**).

## Fourier-Transform Infrared (FTIR)

FTIR spectrum analysis (Figure 2) shows a characteristic absorption band within the ~3400–3200 $cm^{-1}$ region, which reflects the stretching vibration of -NH and -OH groups, indicating that the chitosan and alginate matrices remain intact and hydrated in the NPs α-M HF formulation. The band at around 1640–1650 $cm^{-1}$ (amide I) shows C=O-NH

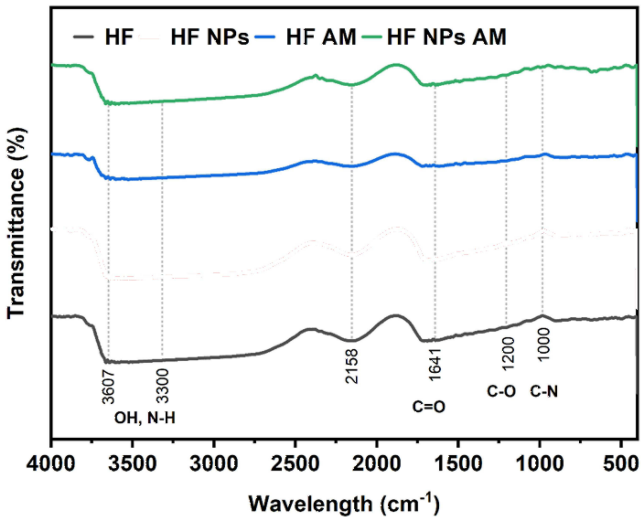


**Figure 2** Comparision of FTIR transmission spectra of HF, HF α-M, and HF α-M NPs.


https://doi.org/10.2147/DDDT.S588115

interactions (amide) indicating the generation of hydrogen bonds between polymers and possible electrostatic interactions between chitosan's amino groups and the carboxylic groups of alginates.

## Weight, Thickness and Degradability Study

The physical features of the hydrogel films were investigated by measuring their weight, thickness, and degradability to assess the structural integrity of the formulations. The thickness of every film was determined utilizing Vernier calipers at 5 different points with 0.001millimeter accuracy, while weights were obtained utilizing an analytical balance, as well as the results are reported as mean ± SEM (n = 5). As shown in Figure 3A and B, incorporation of α-M and its nanoparticle-loaded form resulted in significantly increased film thickness and weight compared with HF alone, indicating enhanced matrix density following active compound incorporation ($p < 0.001$–$0.01$). Degradability studies performed in 20% TCA solution demonstrated that HF α-M and HF α-M NPs exhibited slightly lower degradation percentages relative to HF ($p < 0.001$), suggesting improved structural stability due to the presence of α-M and chitosan–alginate nanoparticles (Figure 3C). Conversely, no notable differences were seen between the formulations when exposed to trypsin (Figure 3D), indicating comparable enzymatic susceptibility across all films. Overall, these findings confirm that the inclusion of α-M, particularly in the nano-encapsulated form, enhances the physicochemical robustness of hydrogel films while maintaining acceptable biodegradability for topical application.

## Mechanical Strength

The mechanical features of the hydrogel films were assessed by evaluating their TS (tensile strength) and EB (elongation at break) in accordance with ASTM D1822 using a Zwick Roell Tensile Tester at a 10 mm/min stretching rate with a 0.05 MPa preload. As shown in Figure 4A and B, HF exhibited the highest TS and EB values, reflecting its flexible and cohesive polymer matrix. The incorporation of α-M induced a notable reduction in TS and EB, suggesting that the direct loading of the hydrophobic compound disrupted polymer chain interactions. However, films containing nano-encapsulated α-M (HF α-M NPs) demonstrated improved TS and EB compared to HF α-M, indicating that nanoparticle incorporation restored matrix uniformity and enhanced load distribution across the films.

## Swelling Degree

The swelling behavior was evaluated by immersing the films in PBS (pH 7.4) and measuring the weight changes over time to calculate the swelling ratio. As depicted in Figure 4C, HF exhibited the highest swelling capacity, consistent with its hydrophilic polymer composition. The addition of α-M significantly reduced the swelling ratio ($p < 0.0001$), likely due to the reduced water affinity and increased film compactness. Hydrogel films incorporating α-M NPs displayed intermediate swelling behavior, with greater fluid uptake than HF α-M but less than HF alone, suggesting that nanoparticle incorporation partially restored hydration capacity while maintaining structural stability. Overall, the mechanical and swelling profiles

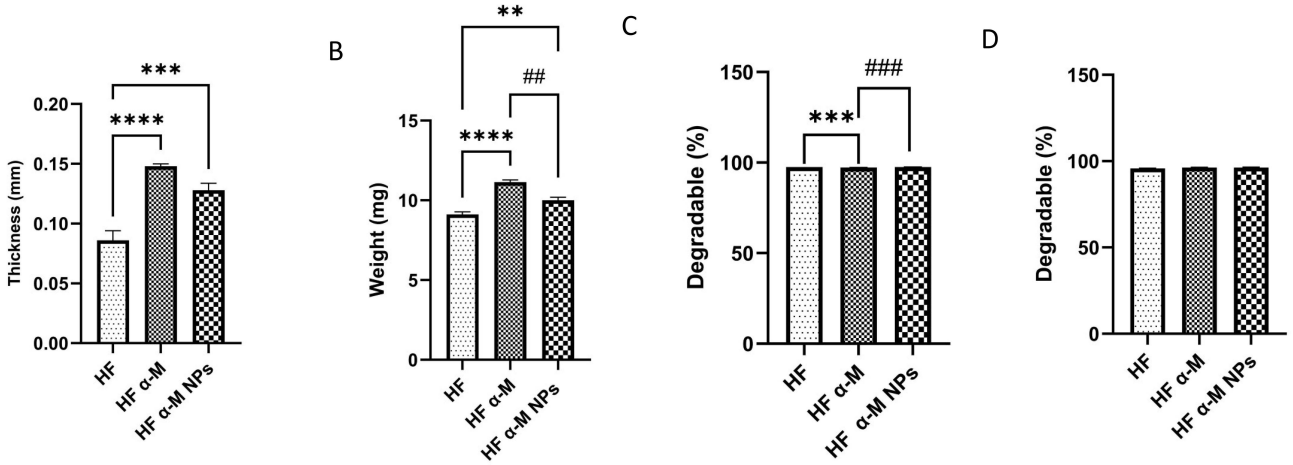


**Figure 3** The thickness (**A**), weight (**B**), The degradable with TCA (**C**) and Trypsin (**D**) of HF, HF α-M, HF α-M NPs. The data were expressed as the mean ± SEM. **p<0.01; ***p<0.001; ****p<0.0001, significant difference compared with the HF. ##p<0.01; ###p<0.001, significant difference compared with the HF α-M (n=5).


https://doi.org/10.2147/DDDT.S588115

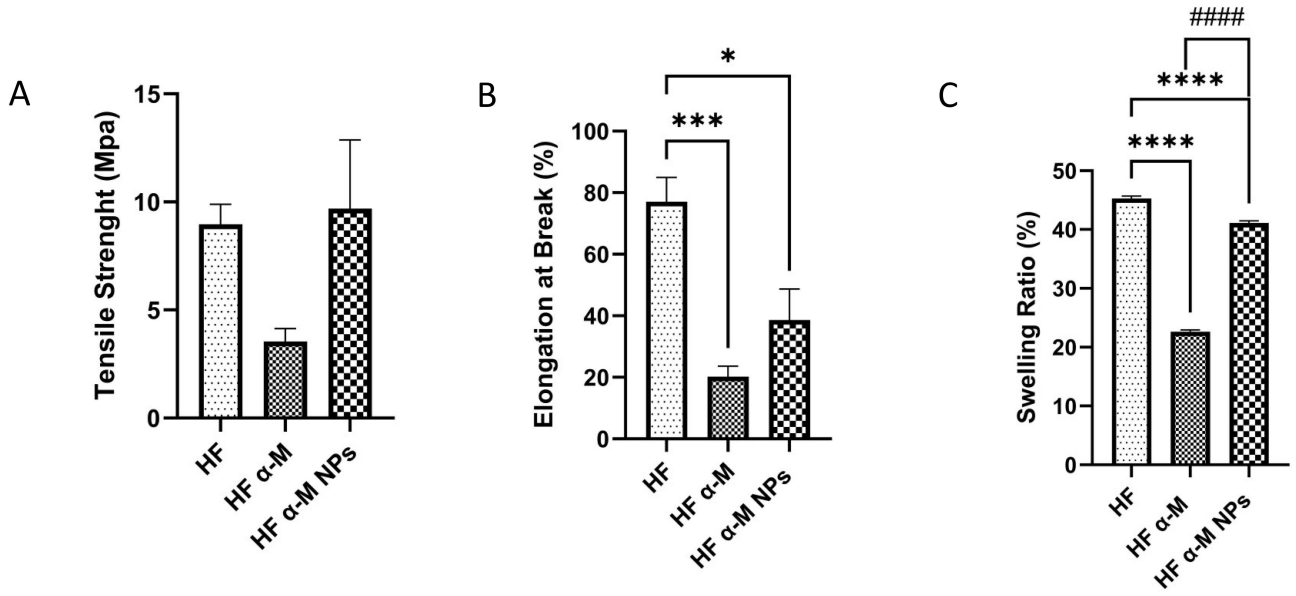


**Figure 4** Mechanical Strength Tensile Strength (**A**), Elongation at Break (**B**), Swelling ratio (**C**) of HF, HF α-M, HF α-M NPs. The data were expressed as the mean ± SEM. *p<0.01; ***p<0.001; ****p<0.0001, significant difference compared with the HF. ####p<0.0001, significant difference compared with the HF α-M (n=5).

indicate that nanoencapsulation enables the integration of α-M into hydrogel films with minimal compromise of film elasticity, strength, and fluid absorption properties, supporting their suitability for topical drug delivery.

## In vitro Release Study

An in vitro release study was executed using the paddle-over-disk method (USP Apparatus V) to characterize the release kinetics of α-M from the different hydrogel film formulations. Dry films of defined thickness and weight were affixed onto glass plates using a bonding agent and soaked in a 500-mL volume of phosphate buffer (pH 7.4) regulated at 32 ± 0.5 °C. The paddle was positioned 2.5 cm above the film surface and was operated at 50 rpm to ensure uniform agitation. Aliquots (5 mL) were drawn at predefined intervals over 270 min as well as immediately substituted with fresh buffer to maintain sink conditions, after which the α-M content was quantified using a UV spectrophotometer at 246 nm. As illustrated in Figure 5, HF α-M exhibited a moderate release profile, whereas free α-M showed minimal diffusion owing to its poor aqueous solubility. In contrast, HF α-M NPs demonstrated a markedly enhanced and sustained release, reaching the highest cumulative percentage over the study period. These results indicate that nanoencapsulation within the chitosan-alginate matrix significantly improved α-M release efficiency, supporting its potential for controlled topical delivery.

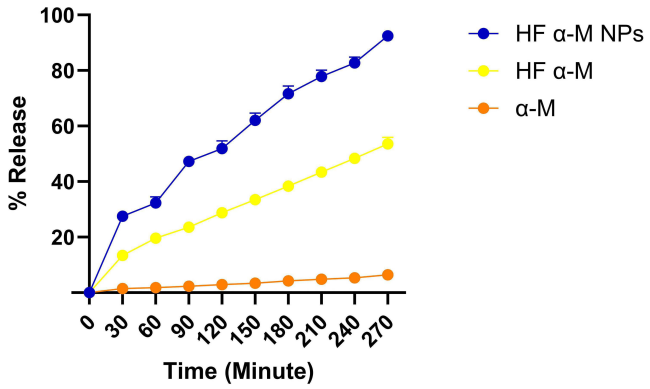


**Figure 5** In vitro release of α-M, HF α-M, HF α-M NPs. The data were expressed as the mean ± SEM (n=5).


https://doi.org/10.2147/DDDT.S588115

## In vivo Antimicrobial Activity

In vivo antimicrobial evaluation demonstrated that the acne model was reliably established in all *P. acnes*-induced groups, as evidenced by progressive skin thickening, erythema, swelling, induration, and nodule formation after three days of intradermal bacterial injection. The subsequent four-day, twice-daily application of the hydrogel formulations resulted in distinguishable therapeutic responses among the treatment groups. Rats treated with HF α-M and HF α-M NPs exhibited visibly attenuated inflammatory manifestations compared to those in the negative control, which received only the hydrogel base. The positive control group administered clindamycin gel showed notable clinical improvement; however, HF α-M NPs produced comparable or greater reductions in papule size and erythema, suggesting enhanced antimicrobial performance of the nano encapsulated formulation. Quantitative analysis using total plate counts corroborated the visual clinical findings. As shown in Table 5, the negative control group exhibited the highest bacterial load ($2.31 \times 10^3$ CFU/g), confirming persistent colonization by *P. acnes*. Treatment with Clindamycin gel reduced the bacterial count to $2.21 \times 10^1$ CFU/g, whereas HF α-M produced a more modest reduction ($2.46 \times 10^2$ CFU/g). Notably, the HF α-M NPs demonstrated the most pronounced antimicrobial effect, yielding the lowest viable bacterial count of $2.46 \times 10^1$ CFU/g, approaching that of the positive control. Gram-positive staining confirmed the presence of *P. acnes* colonies, and all counts were within the acceptable range of 30–300 CFU. These findings indicate that nanoencapsulation of α-M substantially enhanced its in vivo antibacterial activity against *P. acnes* when delivered via a topical hydrogel film.

### Histopathological Evaluation and Skin Irritation Parameters

Histopathological examination of *P. acnes*-induced papules revealed clear and treatment-dependent differences in inflammatory severity and tissue restoration following hematoxylin and eosin staining. As shown in Figure 6A, the negative control (NC) group exhibited severe epithelial disorganization, reflecting extensive tissue damage. This structural deterioration was accompanied by pronounced inflammatory cell infiltration, as evidenced by significantly elevated monocyte (Figure 6B) and lymphocyte counts (Figure 6C), abundant polymorphonuclear cells (Figure 6D), increased neovascularization (Figure 6E), and a marked reduction in fibroblast density (Figure 6F), collectively indicating an unresolved inflammatory state.

In contrast, treatment with clindamycin gel (positive control, PC) resulted in partial normalization of epithelial architecture (Figure 6A) and a noticeable reduction in inflammatory cell infiltration, including monocytes (Figure 6B), lymphocytes (Figure 6C), and polymorphonuclear cells (Figure 6D). This improvement was accompanied by moderated neovascularization (Figure 6E) and increased fibroblast presence (Figure 6F), indicating effective suppression of inflammation and initiation of tissue repair.

Application of HF α-M produced moderate histological improvement. While reductions in monocyte (Figure 6B) and polymorphonuclear cell infiltration (Figure 6D) were observed compared with the negative control, epithelial thickening and incomplete structural organization remained evident (Figure 6A). Moreover, lymphocyte infiltration (Figure 6C), neovascularization (Figure 6E), and fibroblast density (Figure 6F) suggested that the anti-inflammatory effect of free α-M was present but limited.

Notably, the HF α-M NPs group demonstrated the most pronounced and consistent histological recovery among all treated groups. Skin sections showed a well-organized epithelial layer (Figure 6A), a marked reduction in monocytes

**Table 5** Total Plate Count (ALT) Values

| Group | Total Plate Count (CFU/g) |
|---|---|
| Negative Control | $2.31 \times 10^3$ CFU/g |
| Positive Control | $2.21 \times 10^1$ CFU/g |
| HF α-M | $2.46 \times 10^2$ CFU/g |
| HF α-M NPs | $2.46 \times 10^1$ CFU/g |


https://doi.org/10.2147/DDDT.S588115

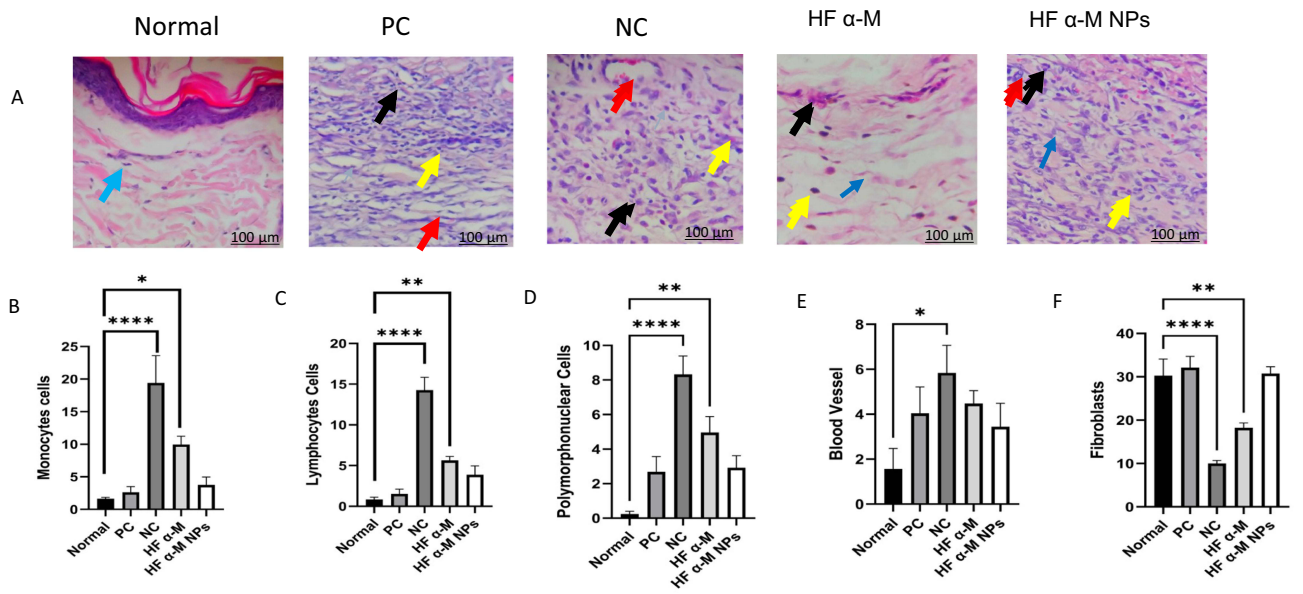


**Figure 6** Skin histopathology among these groups of Histological analysis of skin tissue by hematoxylin and eosin staining magnification of 100 X (**A**). Expression levels of the serum inflammatory factors monocytes cells (**B**), lymphocytes cells (**C**), polymorphonuclear cells (**D**), blood vessel (**E**), fibroblasts (**F**). Light blue arrows: Fibroblast; Yellow arrows: Mononuklear MN; Black arrows: Polimorfonuklear; Red arrows: Blood vessel. The data were expressed as the mean ± SEM. *p<0.05; **p<0.01; ****p<0.0001, significant difference compared with the normal (n=5).

(Figure 6B), lymphocytes (Figure 6C), and polymorphonuclear cells (Figure 6D), along with diminished neovascularization (Figure 6E) and a substantial increase in fibroblast abundance (Figure 6F). Importantly, these changes closely resembled normal skin morphology, highlighting the superior ability of nanoparticle-loaded α-M to simultaneously suppress inflammation and promote tissue regeneration.

Consistent with these histopathological findings, skin irritation parameters are summarized in Figure 7. Representative histological images (Figure 7A) further confirmed reduced tissue disruption in the HF α-M NPs group. Quantitative scoring demonstrated that the negative control group exhibited the highest edema (Figure 7B) and erythema

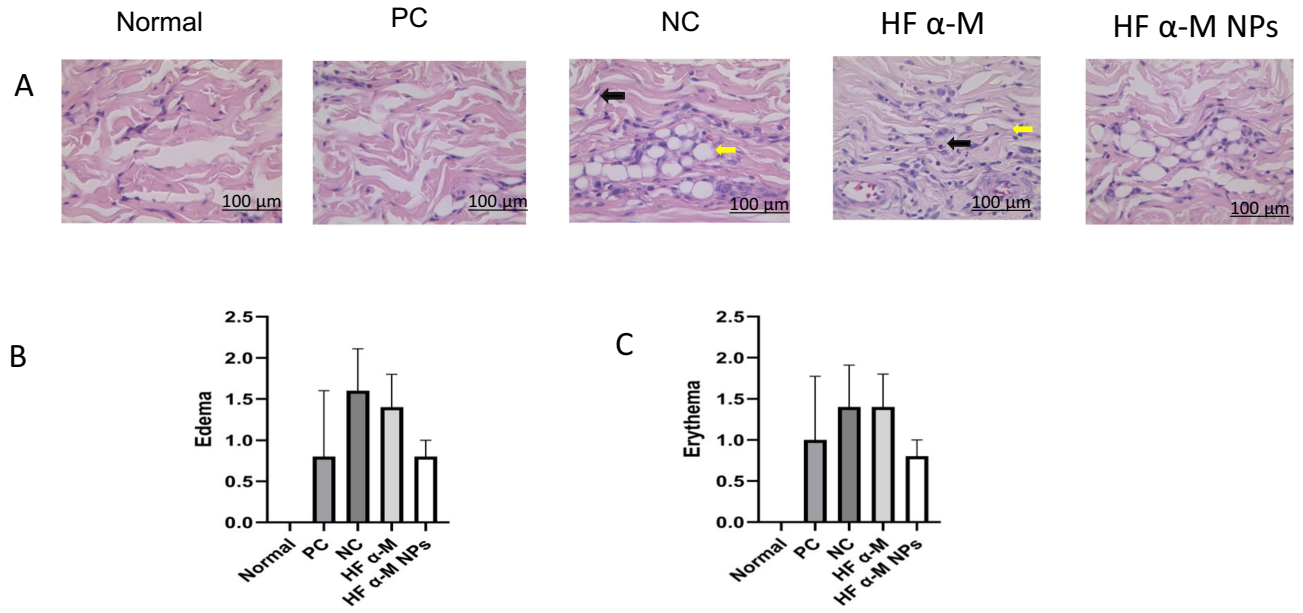


**Figure 7** Skin histopathology among these groups; Histological analysis of skin tissue by hematoxylin and eosin staining magnification of 100 X (**A**). Disease scoring of Edema (**B**). Score of Erythema (**C**). Yellow arrows: Edema; Black arrows: Erythema. The data were expressed as the mean ± SEM.


https://doi.org/10.2147/DDDT.S588115

(Figure 7C). While clindamycin gel and HF α-M treatments produced moderate reductions in both parameters, the HF α-M NPs group showed the lowest edema and erythema scores among all treated groups (Figure 7B and 7C). These results underscore the novelty of incorporating α-M into a nanoparticle-based hydrogel film, which significantly enhances its anti-inflammatory efficacy and accelerates tissue repair compared with free drug and conventional topical treatment.

## Discussion

Chitosan stabilization using polyanions, such as sodium tripolyphosphate (TPP), plays a critical role in producing mechanically stronger and structurally stable nanoparticles suitable for topical delivery systems.[7] The dissolution of chitosan in an acidic medium converts the amine groups ($-NH_2$) into protonated ammonium groups ($-NH_4^+$), which may produce weak and unstable nanoparticle complexes when unbound. The addition of sodium TPP effectively crosslinks these positively charged groups, stabilizing the resulting nanoparticles and enabling optimal encapsulation of α-M.[31] Preparation via ionic gelation exploits the electrostatic interactions between chitosan and TPP, and alginate coating provides additional structural reinforcement. The cationic nature of chitosan further enhances its interactions with the negatively charged bacterial membrane of *P. acnes*, thereby improving its antibacterial potential.[26,54] This stabilization is essential for preventing particle aggregation during storage and use, preserving the bioactivity of α-M, and maintaining the therapeutic consistency of the formulation.

Physicochemical characterization supported the successful formation of chitosan-alginate-based α-M nanoparticles suitable for topical administration. SEM revealed evenly distributed small spherical particles on the HF α-M NPs surface, confirming the effective encapsulation and homogeneous dispersion of α-M within the polymer network.[39,55] This uniformity is crucial because it contributes to enhanced film stability, consistent drug loading, and more predictable drug release behavior compared to the free α-M film, which exhibits surface roughness and aggregated crystals. FTIR analysis further supported the molecular incorporation of α-M, as demonstrated by the shift and intensity changes in the carbonyl region (~1710–1720 $cm^{-1}$), indicating interactions beyond simple physical mixing and preservation of α-M chemical integrity, which is essential for maintaining its antimicrobial efficacy.[40] Macroscopically, the HF α-M NPs exhibited a homogenous color, clarity, and elasticity, reflecting stable polymer-drug interactions that prevent brittleness and maintain film cohesion during application.[7]

These structural and physicochemical attributes translate into functional performance in terms of swelling behavior, mechanical strength, and degradation. Free α-M disrupted the polymer chain alignment, leading to reduced tensile strength and elasticity; however, nanoencapsulation mitigated these undesirable effects by restoring uniformity to the matrix, resulting in improved TS and EB values. The swelling degree of the HF α-M NPs, which was intermediate between that of HF and HF α-M, reflects a balanced hydration capacity that supports drug release while preserving film integrity, an essential attribute for hydrogel patches intended for sustained topical delivery.[39,55] The reduced degradation of TCA by HF α-M and HF α-M NPs indicates increased structural robustness, likely due to polymer drug network reinforcement, whereas similar trypsin-based degradation across all formulations confirms that biodegradability is appropriate for topical biomedical films.

The enhanced performance of the nano-encapsulated α-M was further reflected in the in vivo and in vitro antimicrobial evaluations. The total plate count indicated that α-M produced the greatest reduction in *P. acnes* ($2.46 \times 10^1$ CFU/g), approaching the efficacy of clindamycin gel and outperforming both free α-M and the hydrogel base. These results are consistent with the well-recognized advantages of nanoparticles in improving cutaneous penetration, stability, and localized retention of poorly soluble compounds such as α-M.[45,55] The chitosan-alginate matrix also provides antibacterial and permeation enhancing properties, complementing the inherent antimicrobial activity of α-M. Together, these findings support that nanoencapsulation provides synergistic enhancement of α-M bioactivity, confirming its therapeutic potential for topical acne management.[54]

Histopathological evaluation demonstrated that HF α-M NPs yielded the most significant reduction in inflammatory cell infiltration, improved fibroblast abundance, and restored epithelial organization compared with the other treatment groups. These tissue improvements corresponded directly with the marked decreases in edema and erythema scores, which were the lowest among all *P. acnes* challenged groups, underscoring the superior anti-inflammatory performance of the nanoparticle-loaded hydrogel film.[56–58] In contrast, the negative control exhibited severe inflammatory responses,

reflected by extensive monocyte and polymorphonuclear infiltration and the highest edema-erythema scores. HF α-M produced moderate improvements consistent with a partial reduction of inflammation, whereas clindamycin gel delivered effective but comparatively less pronounced tissue restoration than HF α-M NPs. The strong concordance between histopathology, irritation scores, and bacterial load reduction indicates that nanoencapsulation significantly enhances the pharmacological impact of α-M, supporting improved tissue repair and attenuation of *P. acnes-induced* inflammation.

## Conclusion

This study demonstrated that nanoencapsulation of α-M within a chitosan–alginate matrix effectively improved its physicochemical properties, drug release performance, and therapeutic efficacy for topical acne management. The developed hydrogel films showed favorable structural features, uniform nanoparticle distribution, and well-maintained molecular interactions, supporting sustained α-M delivery. In vivo evaluations confirmed that HF α-M NPs exhibited superior antimicrobial activity against P. acnes, attenuated inflammatory responses, and enhanced epithelial regeneration, outperforming free α-M formulations and achieving therapeutic effects comparable to clindamycin gel. Overall, these findings indicate that chitosan-alginate nano-encapsulated α-M hydrogel films represent a promising alternative topical therapy for acne, offering controlled drug release and anti-inflammatory benefits. Further investigations, including long-term formulation performance, clinical validation, and scale-up optimization, are required to facilitate the translation of this formulation into clinical and commercial applications.

## Acknowledgments

The authors would like to acknowledge the Rector of Universitas Padjadjaran through the Indonesian Endowment Fund for Education (LPDP), under the Ministry of Higher Education, Science, and Technology of Indonesia, and managed under the EQUITY Program (Contract No. 4303/ 83/ DT.03.08/ 2025 and 3927/ UN6. RKT/HK.07.00/2025).

## Funding

The APC is funded by Universitas Padjadjaran through the EQUITY Program.

## Disclosure

The authors declare no conflicts of interest in this work.

## References

1. Chen SY, Wang ZQ, Tang Q, et al. Metabolomic profiling reveals distinct plasma metabolic signatures in acne patients with and without depression. *Clin CosmetInvest Dermatol*. 2025;29:2923–2937.
2. Annunziata MC, Potestio L, Napolitano M, Napolitano M. Efficacy and safety of hormonal therapies for acne: a narrative review. *Clin Cosmet Investigat Dermatol*. 2025;18:3331–3337. doi:10.2147/CCID.S574341
3. Chakraborty N, Narayanan V, Gautam HK. Nano-therapeutics to treat acne vulgaris. *Indian J Microbiol*. 2022;62(2):167–174. doi:10.1007/s12088-022-01001-4
4. Abid F, Kim S, Savaliya B, et al. Targeting acne: development of monensin-loaded nanostructured lipid carriers. *Int J Nanomed*. 2025;20:2181–2204. doi:10.2147/IJN.S497108
5. Phumlek K, Itharat A, Pongcharoen P, et al. Garcinia mangostana hydrogel patch: bactericidal activity and clinical safety for acne vulgaris treatment. *Res Pharm Sci*. 2022;17(5):457–467. doi:10.4103/1735-5362.355195
6. Pan-In P, Wongsomboon A, Kokpol C, Chaichanawongsaroj N, Wanichwecharungruang S. Depositing α-mangostin nanoparticles to sebaceous gland area for acne treatment. *J Pharmacol Sci*. 2015;129(4):226–232. doi:10.1016/j.jphs.2015.11.005
7. Wathoni N, Rusdin A, Motoyama K, Joni IM, Lesmana R, Muchtaridi M. Nanoparticle drug delivery systems for α-mangostin. *Nanotechnol Sci Appl*. 2020;13:23–36. doi:10.2147/NSA.S243017
8. Wathoni N, Rusdin A, Febriani E, et al. Formulation and characterization of α-mangostin in chitosan nanoparticles coated by sodium alginate, sodium silicate, and polyethylene glycol. *J Pharm Bioallied Sci*. 2019;11(8):S619–S627. doi:10.4103/jpbs.JPBS_206_19
9. Raszewska-Famielec M, Flieger J. Nanoparticles for topical application in the treatment of skin dysfunctions—an overview of dermo-cosmetic and dermatological products. *Int J Mol Sci*. 2022;23(24). doi:10.3390/ijms232415980
10. Sriviriyakul K. Clinical efficacy of topical mangosteen extract nanoparticle loaded gel compared with 1 % clindamycin gel in mild to moderate acne vulgaris clinical efficacy of topical mangosteen extract nanoparticle loaded gel compared with 1 % clindamycin gel in mild T; 2016.
11. Tanngoen P, Lamlertthon S, Tiyaboonchai W. Characterization and evaluation of α-mangostin-loaded film-forming gels for acne treatment. *Indian J Pharm Sci*. 2020;82(1):157–165. doi:10.36468/pharmaceutical-sciences.633
12. Makhmalzade BS, Chavoshy F. Polymeric micelles as cutaneous drug delivery system in normal skin and dermatological disorders. *J Adv Pharm Technol Res*. 2018;9(1):2–8. doi:10.4103/japtr.JAPTR_314_17

13. Kapoor MS, Guhasarkar S, Banerjee R. Stratum corneum modulation by chemical enhancers and lipid nanostructures: implications for transdermal drug delivery. *Ther Deliv*. 2017;8(8):701–718. doi:10.4155/tde-2017-0045
14. Ahmad Nasrollahi S, Koohestani F, Naeimifar A, Samadi A, Vatanara A, Firooz A. Preparation and evaluation of Adapalene nanostructured lipid carriers for targeted drug delivery in acne. *Dermatol Ther*. 2021;34(2):1–10. doi:10.1111/dth.14777
15. Jain A, Garg NK, Jain A, et al. A synergistic approach of Adapalene-loaded nanostructured lipid carriers, and vitamin C co-administration for treating acne. *Drug Dev Ind Pharm*. 2016;42(6):897–905. doi:10.3109/03639045.2015.1104343
16. Chutoprapat R, Witarat J, Jongpanyangarm P, Mang Sung Thluai L, Khankaew P, Wah Chan L. Development of solid lipid microparticles (SLMs) containing asiatic acid for topical treatment of acne: characterization, stability, in vitro and in vivo anti-acne assessment. *Int J Pharm*. 2024;654:123980. doi:10.1016/j.ijpharm.2024.123980
17. Pornpattananangkul D, Fu V, Thamphiwatana S, et al. In vivo treatment of propionibacterium acnes infection with liposomal lauric acids. *Adv Healthc Mater*. 2013;2(10):1322–1328. doi:10.1002/adhm.201300002
18. Ag Seleci D, Seleci M, Walter JG, Stahl F, Scheper T. Niosomes as nanoparticular drug carriers: fundamentals and recent applications. *J Nanomater*. 2016;2016(Figure 1):1–13. doi:10.1155/2016/7372306
19. Zanganeh SM. Preparation and characterization of Chitosan- Alginate biopolymer loaded by clindamycin phosphate as an effective drug delivery system for the treatment of Acne; 2023:1–20.
20. Wathoni N, Yuniarsih N, Cahyanto A, Muhctaridi M. A-mangostin hydrogel film based chitosan-alginate for recurrent aphthous stomatitis. *Appl Sci*. 2019;9(23):5235. doi:10.3390/app9235235
21. Wathoni N, Suhandi C, Purnama MFG, et al. Alginate and chitosan-based hydrogel enhance antibacterial agent activity on topical application. *Infect Drug Resist*. 2024;17:791–805. doi:10.2147/IDR.S456403
22. Abd-allah H, Abdel-aziz RTA, Nasr M. International Journal of Biological Macromolecules Chitosan nanoparticles making their way to clinical practice: a feasibility study on their topical use for acne treatment. *Int J Biol Macromol*. 2020;156:262–270. doi:10.1016/j.ijbiomac.2020.04.040
23. Nasrul W, Lisna M, Agus Rusdin AFAM, et al. Alpha mangostin chitosan nanoparticle loaded kappa carrageenan improves cytotoxic effect of -mangostin on MCF-7 cell line. *Nanotechnol Sci Appl*. 2020;5:1–19.
24. Vitamia C, Iftinan GN, Latarissa IR, et al. α-Mangostin hydrogel film with chitosan alginate base for recurrent aphthous stomatitis (RAS) treatment: study protocol for double-blind randomized controlled trial. *Front Pharmacol*. 2024;15:1–7. doi:10.3389/fphar.2024.1353503
25. Haque T, Talukder MU. Chemical enhancer: a simplistic way to modulate barrier function of the stratum corneum. *Advanced Pharmaceutical Bulletin*. 2018;8(2):169–179. doi:10.15171/apb.2018.021
26. Marwah H, Garg T, Goyal AK, Rath G. Permeation enhancer strategies in transdermal drug delivery. *Drug Deliv*. 2016;23(2):564–578. doi:10.3109/10717544.2014.935532
27. Kapao N, Wattanutchariya W, Hamontree C. Development of natural acne patch from local materials using quality function deployment technique. *MATEC Web Conf*. 2018;192:4–7. doi:10.1051/matecconf/201819201050
28. Kuo CW, Chiu YF, Wu MH, et al. Gelatin/chitosan bilayer patches loaded with cortex phellodendron amurense/centella asiatica extracts for anti-acne application. *Polymers*. 2021;13(4):1–15. doi:10.3390/polym13040579
29. Qothrunnadaa T, Hasanah AN. Patches for Acne Treatment: an Update on the Formulation and Stability Test. *Int J Appl Pharm*. 2021;13(Special Issue 4):21–26. doi:10.22159/IJAP.2021.V13S4.43812
30. Ibrahim HK, Sorour RMH, Salah Ad-din I. Application of mathematical modelling to alginate chitosan polyelectrolyte complexes for the prediction of system behavior with Venlafaxine HCl as a model charged drug. *Saudi Pharm J*. 2022;30(10):1507–1520. doi:10.1016/j.jsps.2022.07.013
31. Yuniarsih N, Chaerunisaa AY, Elamin KM, Wathoni N. Polymeric nanohydrogel in topical drug delivery system. *Int J Nanomed*. 2024;19:2733–2754. doi:10.2147/IJN.S442123
32. Guo L, Liang Z, Yang L, et al. The role of natural polymers in bone tissue engineering. *J Control Release*. 2021;338:571–582. doi:10.1016/j.jconrel.2021.08.055
33. Chen H, Lu Q, Cao X, Wang N, Wang ZL. Natural polymers based triboelectric nanogenerator for harvesting biomechanical energy and monitoring human motion. *Nano Res*. 2022;15(3):2505–2511. doi:10.1007/s12274-021-3764-6
34. Claudio C, Giuffrida R, Fadda S, et al. Topical dermocosmetics and acne vulgaris. *Dermatol Clin*. 2021;34(1):e14436.
35. Park SY, Lee JH, Ko SY, Kim N, Kim SY, Lee JC. Antimicrobial activity of α-mangostin against Staphylococcus species from companion animals in vitro and therapeutic potential of α-mangostin in skin diseases caused by S. pseudintermedius. *Front Cell Infect Microbiol*. 2023;13:1–14. doi:10.3389/fcimb.2023.1203663
36. Alhakamy NA, Neamatallah T, Alshehri S, Mujtaba A. α -mangostin-loaded polymeric nanoparticle gel for topical therapy in skin cancer. *Gels*. 2021;7(230):1–26.
37. Rudyardjo DI, Wijayanto S. The synthesis and characterization of hydrogel chitosan-alginate with the addition of plasticizer lauric acid for wound dressing application. *J Phys Conf Ser*. 2017;853(1):012042. doi:10.1088/1742-6596/853/1/012042
38. Gaber DA, Alburaykan AI, Alruthea LM, et al. Development, in vitro evaluation, and in vivo study of adhesive buccal films for the treatment of diabetic pediatrics via trans mucosal delivery of gliclazide. *Drug Design, Development and Therapy*. 2022;16:4235–4250. doi:10.2147/DDDT.S394523
39. Sulastri E, Zubair MS, Lesmana R, Wathoni N, Wathoni N. Development and characterization of ulvan polysaccharides-based hydrogel films for potential wound dressing applications. *Drug Design, Development and Therapy*. 2021;15:4213–4226. doi:10.2147/DDDT.S331120
40. Rohman A, Arifah FH, Irnawati, Alam G, Muchtaridi M. The application of FTIR spectroscopy and chemometrics for classification of Mangosteen extract and its correlation with alpha-mangostin. *J Appl Pharm Sci*. 2020;10(4):149–154. doi:10.7324/JAPS.2020.104019
41. Wathoni N, Hasanah AN, Mohammed AFA, Pratiwi ED, Mahmudah R. Accelerated wound healing ability of sacran hydrogel film by keratinocyte growth factor in alloxan-induced diabetic mice. *Int J Appl Pharm*. 2018;10(2):57–61. doi:10.22159/ijap.2018v10i2.24217
42. Dubey A. Formulation and characterization of anti-epileptic drug biomedical European of and pharmaceutical sciences; 2021.
43. Bailey J, Oliveri A, Levin E. 基因的改变NIH Public Access. *Bone*. 2013;23(1):1–7. doi:10.1002/adhm.201300002.In
44. Liu RJ, Li M, Zhu Q, et al. Development and characterization of a hydrogel containing chloramphenicol-loaded binary ethosomes for effective transdermal permeation and treatment acne in rat model. *Int J Nanomed*. 2025;20:1697–1715. doi:10.2147/IJN.S476937
45. Agarwal P, Tyagi N, Gaur PK, Puri D, Shanmugam SK. Polyherbal anti acne gel containing extracts of *Mangifera indica* and *Syzygium cumini* seeds: bioassay guided activity against Propionibacterium acne. *Biointerface Res Appl Chem*. 2019;9(4):4177–4182. doi:10.33263/BRIAC94.177182

46. Hossain TJ. Methods for screening and evaluation of antimicrobial activity: a review of protocols, advantages, and limitations. *Eur J Microbiol Immunol*. 2024;14(2):97–115. doi:10.1556/1886.2024.00035
47. Bankier C, Cheong Y, Mahalingam S, et al. A comparison of methods to assess the antimicrobial activity of nanoparticle combinations on bacterial cells. *PLoS One*. 2018;13(2):1–13. doi:10.1371/journal.pone.0192093
48. Hemmati M, Ghasemzadeh A, Malek-Kheili MH, Khoshnevisan K, Koohi MK. Investigation of acute dermal irritation/corrosion, acute inhalation toxicity and cytotoxicity tests for Nanobiocide. *Nanomedicine Res J*. 2016;1(1):23–29. doi:10.7508/NMRJ.2016.01.004
49. Majumder R, Adhikari L, Dhara M, Sahu J. Evaluation of anti-inflammatory, analgesic and TNF-α inhibition (upon RAW 264.7 cell line) followed by the selection of extract (leaf and stem) with respect to potency to introduce anti-oral-ulcer model obtained from Olax psittacorum (Lam.) Vahl in additi. *J Ethnopharmacol*. 2020;263:113146. doi:10.1016/j.jep.2020.113146
50. Milanda T, Cindana Mo'o FR, Mohammed AFA, et al. Alginate/chitosan-based hydrogel film containing α-mangostin for recurrent aphthous stomatitis therapy in rats. *Pharmaceutics*. 2022;14(8):1709. doi:10.3390/pharmaceutics14081709
51. Roberts MS, Cheruvu HS, Mangion SE, et al. Topical drug delivery: history, percutaneous absorption, and product development. *Adv Drug Deliv Rev*. 2021:177. doi:10.1016/j.addr.2021.113929
52. Parhi R, Sahoo SK, Das A. Drug transport pathways across skin; 2022.
53. Ramanunny AK, Wadhwa S, Gulati M, et al. Nanocarriers for treatment of dermatological diseases: principle, perspective and practices. *Eur J Pharmacol*. 2021:890. doi:10.1016/j.ejphar.2020.173691
54. Verma S, Utreja P, Kumar L. Nanotechnological carriers for treatment of acne. *Bentham Sci*. 2018;13(2):105–126. doi:10.2174/1574891X13666180918114349
55. Treenate P, Monvisade P, Yamaguchi M. Development of hydroxyethylacryl chitosan/alginate hydrogel films for biomedical application. *J Polym Res*. 2014;21(12):1–12. doi:10.1007/s10965-014-0601-6
56. Sibero HT, Darwin E, Wirasati Y, Yenny SW. The difference in interleukin-8 (IL-8) on degrees of acne vulgaris severity. *Indian J Foren Med Toxicol*. 2021;15(3):3207–3212.
57. Design D. Network pharmacology and experimental validation to explore the molecular mechanisms of compound huangbai liquid for the treatment of acne. *Drug Design Dev ther*. 2023;31:39–53.
58. Ouyang X, Li C, Zhu S. Untargeted lipidomics analysis to discover lipid profiles and biomarkers of rabbit acne model and reveal action mechanism of isotretinoin. *Drug design, Development and Therapy*. 2024;18:4003–4016. doi:10.2147/DDDT.S476649